AWARD NUMBER: W81XWH-13-1-0238

TITLE: Developing Inhibitors of Translesion DNA Synthesis as Therapeutic Agents Against Lung Cancer

PRINCIPAL INVESTIGATOR: Anthony J. Berdis, Ph.D.

CONTRACTING ORGANIZATION: Cleveland State University
Cleveland, Ohio, 44115

REPORT DATE: October 2014

TYPE OF REPORT: Annual Report

PREPARED FOR: U.S. Army Medical Research and Materiel Command
Fort Detrick, Maryland 21702-5012

REPORT DOCUMENTATION PAGE

Form Approved
OMB No. 0704-0188

1. REPORT DATE	2. REPORT TYPE	3. DATES COVERED
October 2014	Annual	20Sep2013-19Sep2014

4. TITLE AND SUBTITLE: Developing Inhibitors of Translesion DNA Synthesis as Therapeutic Agents against Lung Cancer

5a. CONTRACT NUMBER W81XWH-13-1-0238

5b. GRANT NUMBER

5c. PROGRAM ELEMENT NUMBER

6. AUTHOR(S): Anthony J. Berdis, Ph.D.

email: a.berdis@csuohio edu

5d. PROJECT NUMBER

5e. TASK NUMBER

5f. WORK UNIT NUMBER

7. PERFORMING ORGANIZATION NAME(S) AND ADDRESS(ES)
Cleveland State University
Cleveland, Ohio, 44115

8. PERFORMING ORGANIZATION REPORT

9. SPONSORING / MONITORING AGENCY NAME(S) AND ADDRESS(ES)

U.S. Army Medical Research and Materiel Command
Fort Detrick, Maryland 21702-5012

10. SPONSOR/MONITOR'S ACRONYM(S)

11. SPONSOR/MONITOR'S REPORT NUMBER(S)

12. DISTRIBUTION / AVAILABILITY STATEMENT

Approved for Public Release; Distribution Unlimited

13. SUPPLEMENTARY NOTES

14. ABSTRACT

Oxygen-rich environments can create pro-mutagenic DNA lesions such as 8-oxoguanine (8-oxo-G) that can be misreplicated during translesion DNA synthesis (TLS). Our work has evaluated the pro-mutagenic behavior of 8-oxo-G by quantifying the ability of high-fidelity and specialized DNA polymerases to incorporate natural and modified nucleotides opposite this lesion. We have demonstrated that high-fidelity DNA polymerases (eukaryotic pol delta and bacteriophage T4 DNA polymerase) display error-prone tendencies when replicating 8-oxo-G, they display remarkably low efficiencies for TLS compared to normal DNA synthesis. In contrast, pol eta shows a combination of high efficiency and low fidelity when replicating 8-oxo-G. These combined properties are consistent with a pro-mutagenic role for pol eta when replicating this DNA lesion under cellular conditions. Studies with modified nucleotide analogs indicate that pol eta relies heavily on hydrogen-bonding interactions during normal and translesion synthesis. However, some nucleobase modifications including alkylation to the O^6 and N^2 position of guanine increase error-prone replication of 8-oxo-G. These results have identified two (2) nucleotide analogs that are efficiently and selectively utilized by pol h. We are currently testing the ability of the corresponding nucleoside analogs to act as anti-cancer agents that inhibit the activity of pol eta when replicating damaged DNA.

15. SUBJECT TERMS: Mutagenesis, DNA polymerases, nucleoside analogs, chemotherapeutic agents

16. SECURITY CLASSIFICATION OF:			17. LIMITATION OF ABSTRACT	18. NUMBER OF PAGES	19a. NAME USAMRMC RESPONSIBLE PERSON
a. REPORT	b. ABSTRACT	c. THIS PAGE			19b. TELEPHONE NUMBER
Unclassified	Unclassified	Unclassified	Unclassified	43	

Standard Form 298 (Rev. 8-98)

Table of Contents

1. Introduction: This proposal set out to develop novel nucleoside and nucleotide analogs that possess both *thera*peutic and diag*nostic* activities against lung cancer. These "theranostic" nucleotides were designed to be efficiently and selectively utilized by several DNA polymerases that replicate damaged DNA. After incorporation, these analogs terminate the misreplication of damaged DNA to produce therapeutic effects against lung cancer. The ability to "tag" the nucleotides with fluorogenic moieties via "click" chemistry provides unique diagnostic capabilities to measure their incorporation opposite DNA lesions. The combined therapeutic and diagnostic activities will aid to define the role of pro-mutagenic DNA replication in the development and progression of lung cancer. By terminating the misreplication of damaged DNA, these analogs will help prevent DNA mutagenesis, an underlying cause of lung cancer. This last aspect provides the basis for a new therapeutic strategy against lung cancer that will combine these analogs with existing therapeutic agents that damage DNA. Toward this goal, we have identified two (2) lead nucleotides that are efficiently and selectively incorporated opposite a unique DNA lesion commonly formed under hyperoxic conditions present in the lung.

2. Keywords: Mutagenesis, lung cancer, DNA polymerases, nucleoside analogs, chemotherapeutic agents, chemosensitizers

3. Overall Project Summary:

Objective 1: Synthesis and testing of non-natural nucleotides against specialized DNA polymerases.

Task 1A. Synthesis of 5-substituted indolyl nucleosides and corresponding nucleotides.

We have completed the synthesis and chemical characterization of six (6) distinct nucleotide analogs using our established protocols. Provided below is the synthetic route for one compound designated 3-ethynyl-5-nitroindolyl-2'-deoxynucleoside (Figure 1).

Figure 1. Synthetic scheme for 3-ethynyl-5-nitroindolyl-2'-deoxynucleoside and corresponding nucleoside triphosphate.

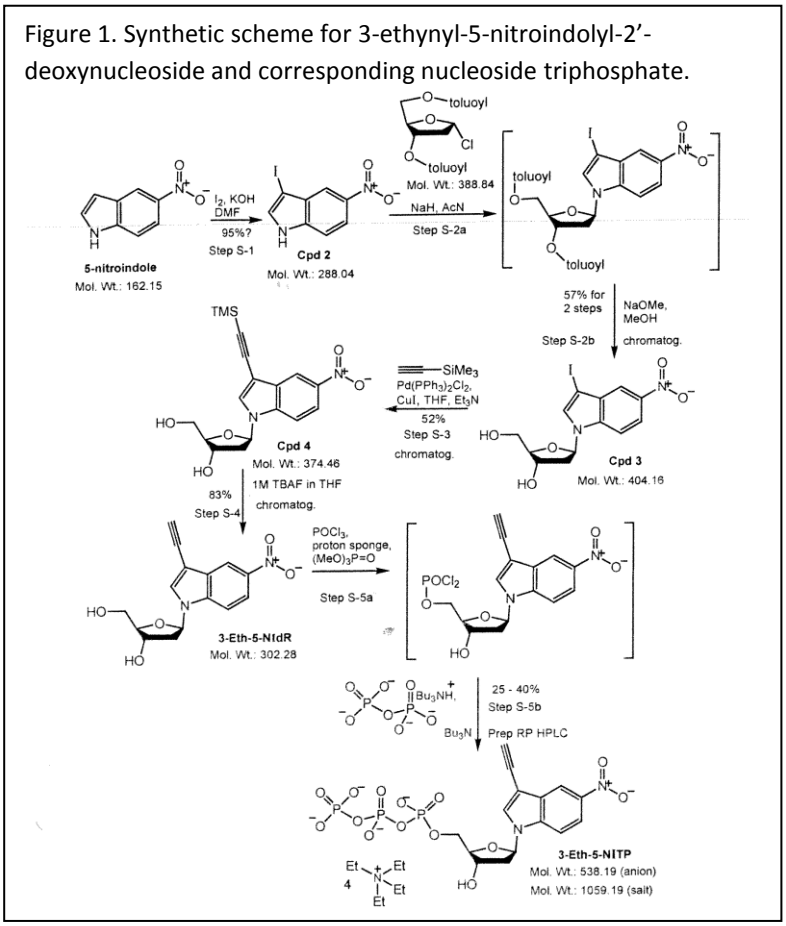

The identity of 3-ethynyl-5-nitroindolyl-2'-deoxynucleoside has been confirmed using LC/MS (liquid chromatography/mass spectroscopy) (Figure 2) and nuclear magnetic resonance (NMR spectroscopy (Figure 3).

Figure 2. Mass spectroscopy to verify the molecular weight of 3-ethynyl-5-nitroindolyl-2'-deoxynucleoside.

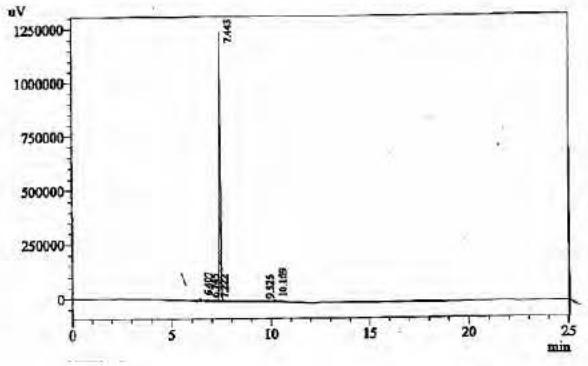

Figure 3. NMR spectrum of 3-ethynyl-5-nitroindolyl-2'-deoxynucleoside.

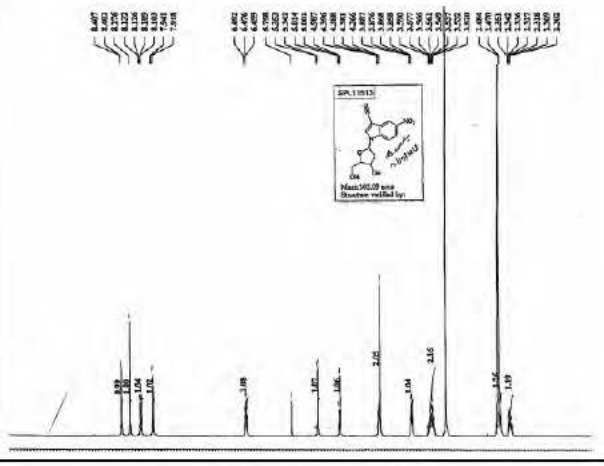

As described below, we have characterized the enzymatic incorporation of these analogs. Results of these studies have generated a structure-activity relationship to further develop additional analogs that are predicted to be both efficient and selective substrates for pol eta during the replication of oxidized DNA lesions. While this task is technically completed, our results validate pursuing the synthesis of at least three (3) additional analogs that will be tested for enzymatic activity as described under **Task 1B**.

Task 1B. Determination of Kinetic Parameters. k_{cat}, K_m, and k_{cat}/K_m values were measured for the aforementioned nucleotide analogs developed in ***Task 1A***. Figures 4 and 5 provides representative Michaelis-Menten plots for the utilization of dATP and N^2-MedGTP during the replication of the oxidized lesion, 8-oxoguanine (8-oxoG) catalyzed by human pol eta (pol η). These kinetic data

Figure 4. Michaelis-Menten plot for the incorporation of dATP opposite 8-oxoguanine (8-oxoG) catalyzed by human pol eta.

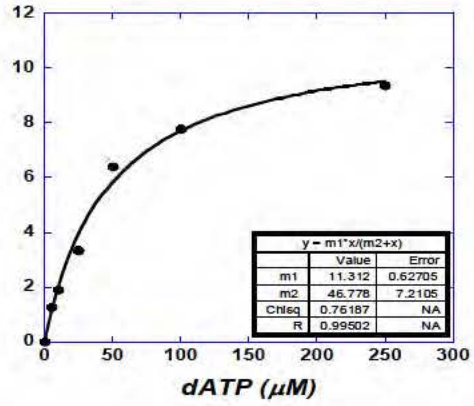

Figure 5. Michaelis-Menten plot for the incorporation of N^2-MedGTP opposite 8-oxoguanine (8-oxoG) catalyzed by human pol eta.

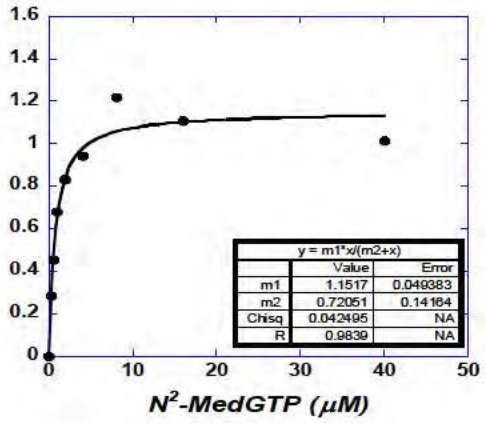

In addition, we measured the kinetic parameters for ten (10) other analogs, several of which were previously synthesized in my laboratory. The kinetic parameters for these analogs are summarized in Tables 1 and 2.

Table 1. Summary of kinetic constants measured for the incorporation of natural and modified nucleotides opposite 8-oxoguanine (8-oxo-G) by pol η.

Nucleotide	K_m (μM)	k_{cat} (sec^{-1})	k_{cat}/K_m ($M^{-1}sec^{-1}$)	Efficiency
dATP	47 +/- 7	1.13 +/- 0.06	(2.4 +/- 0.3)*10^4	100%
N^6-MedATP	46 +/- 15	1.35 +/- 0.15	(2.9 +/- 0.2)*10^4	120%
6-Cl-PTP	137 +/- 7	0.39 +/- 0.08	(2.8 +/- 0.4)*10^3	12%
6-Cl-2APTP	14.3 +/- 3.2	0.09 +/- 0.01	(6.3 +/- 0.6)*10^3	26%
dGTP	32 +/- 10	0.25 +/- 0.03	(7.8 +/- 0.8)*10^3	33%
O^6-MedGTP	50 +/- 15	0.55 +/- 0.13	(1.1 +/- 1.0)*10^4	46%
N^2-MedGTP	**0.64 +/- 0.05**	**0.11 +/- 0.02**	**(1.7 +/- 0.1)*10^5**	**720%**

Table 2. Summary of kinetic constants measured for the incorporation of non-natural nucleotides opposite g 8-oxoguanine by polymerase eta.

Nucleotide	K_m (μM)	k_{cat} (sec^{-1})	k_{cat}/K_m ($M^{-1}sec^{-1}$)	Efficiency
dATP	47 +/- 7	1.13 +/- 0.06	24,000 +/- 3,000	100%
IndTP	61 +/- 18	0.050 +/- 0.005	820 +/- 120	3.4%
5-MeITP	18 +/- 5	0.047 +/- 0.001	2,610 +/- 200	10.9%
5-EtITP	36 +/- 16	0.007 +/- 0.001	200 +/- 50	0.8%
5-EyITP	56 +/- 36	0.0015 +/- 0.0003	27 +/- 15	0.1%
5-NITP	63 +/- 12	0.344 +/- 0.020	5,460 +/- 550	23%
4-NITP	23 +/- 8	0.132 +/- 0.016	5,740 +/- 350	24%
6-NITP	**3.9 +/- 1.6**	**0.283 +/- 0.032**	**72,600 +/- 1,200**	**303%**

These studies have identified two (2) lead compounds highlighted in **bold** that show promising activity as selective and efficient substrates for pol eta. These analogs, N^2-MedGTP and 6-NITP, are incorporated opposite 8-oxoguanine several-fold more efficiently than dATP. As described below, we are in the process of testing the efficacy of the corresponding nucleoside analogs to inhibit pol eta activity under cellular conditions. These studies will ultimately define the potential anti-cancer activities of the nucleoside analogs against lung cancer. Finally, a manuscript describing the results of these studies has been submitted to the scientific journal "*Nucleic Acids Research*". While this task is technically completed, we plan to test the enzymatic activity of the three (3) additional analogs described under **Task 1A** as a pre-requisite to complete **Objectives 2** and **3**.

Task 1C. Evaluating Chain Termination Capabilities. We have investigated the ability of several non-natural nucleotides studied in this project to function as chain-terminating substrates for various DNA polymerases. Representative gel electrophoresis data is provided in Figure 5 and shows interesting results that highlight the ability of pol η to perform pro-mutagenic DNA synthesis

when replicating 8-oxo-G. As illustrated, pol η can easily extend beyond dCMP and dAMP when paired opposite 8-oxo-G. An interesting feature is that pol η easily extends beyond dAMP even in the absence of the next correct nucleotide. This is unusual as this specialized polymerase appears to misinsert dATP opposite A at position 15 of the template. When supplied with the nucleotides needed for elongation, pol η again easily extends beyond both mispaired primers/templates to yield full length product.

Figure 6. Gel electrophoresis data summarizing the incorporation and extension of modified and non-natural nucleotides opposite 8-oxo-G catalyzed by pol eta.

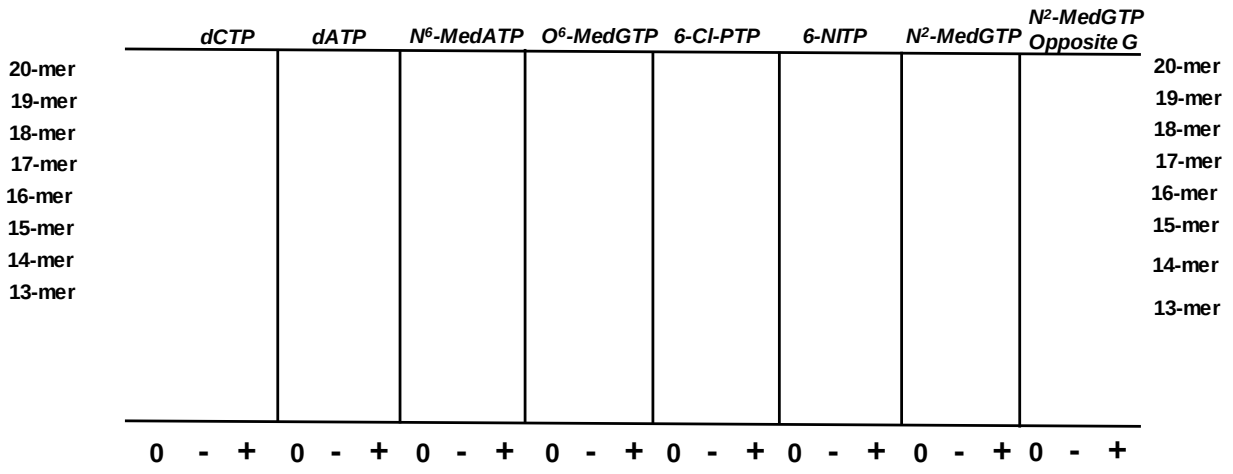

Similar results are obtained when pol η is supplied with modified nucleotides. In particular, pol η easily elongates beyond 6-Cl-PTP, N^6-MedATP, and O^6-MedGTP in the absence of the next correct nucleotide. However, slight differences are observed in the efficiency of elongation when supplied with nucleotides needed for complete elongation of the primer. In this case, the halogenated analog, 6-Cl-PTP is elongated with a higher efficiency compared to either of the alkylated nucleotides, N^6-MedATP and O^6-MedGTP.

6-NITP is incorporated opposite 8-oxo-G and subsequently extended in the absence of complementary dNTPs. However, pol η poorly extends beyond 6-NIMP when supplied with the next correct nucleotides, dTTP and dGTP. This later result is consistent with previous reports demonstrating that high-fidelity DNA polymerases display difficulties in elongating substituted indolyl-nucleotides. Thus, our in vitro data indicates that 6-NITP functions as an efficient chain-terminating nucleotide for pol η. However, the most unusual behavior is that exhibited by N^2-MedGTP. Specifically, pol η efficiently inserts N^2-MedGTP opposite 8-oxo-G and continues to elongate the mispair to positions 17 and 18 of the template. Thus, pol η effectively misinserts N^2-MedGTP opposite a templating adenine (A) and then incorporates opposite two templating cytosine (C) bases before terminating synthesis at the next templating adenine (A). This task is considered complete.

Task 1D. Utilization by Other DNA Polymerases. We have measured the kinetic parameters (k_{cat}, K_m, and k_{cat}/K_m) for the aforementioned nucleotide analogs developed in **Task 1A** using several different DNA polymerases including high fidelity DNA polymerases such as pol δ. Our results summarized below in Tables 3 and 4 indicate that most of our nucleotide analogs behave as poor substrates for high fidelity DNA polymerases involved in chromosomal DNA replication. This validates our conclusion that several of these analogs are selective for the specialized DNA polymerase, pol eta, during the replication of oxidized DNA lesions. This task is complete.

Table 3. Summary of kinetic parameters for the incorporation of modified nucleotides opposite 8-oxoguanine.

dNTP	K_m [μM]	k_{cat} [sec^{-1}]	k_{cat}/K_m [M^{-1} sec^{-1}]	Efficiency
dATP	566 ± 25	0.535 ± 0.015	$1.03 * 10^3$	100 %
2,6-APTP	1,370 ± 410	0.787 ± 0.156	$0.5 * 10^3$	50 %
dITP	28 ± 8	0.008 ± 0.005	$2.9 * 10^2$	27 %
6-Cl-PTP	51 ± 17	0.0123 ± 0.0007	$2.31 * 10^2$	15 %
6-Cl-2APTP	145 ± 33	0.049 ± 0.004	$3.37 * 10^2$	22 %
dGTP	*No insertion*			NA
N^6-MedATP	135 ± 41	0.056 ± 0.005	$4.14 * 10^2$	18 %
O^6-MedGTP	82 ± 11	0.023 ± 0.001	$2.79 * 10^2$	19 %
N^2-MedGTP	*No insertion*			NA

Table 4. Summary of kinetic parameters for the incorporation of non-natural nucleotides opposite 8-oxoguanine.

dNTP [μM]	K_m [μM]	k_{cat} [sec^{-1}]	k_{cat}/K_m [M^{-1} sec^{-1}]	Efficiency
dATP	566 ± 25	0.535 ± 0.015	$1.5 * 10^3$	100 %
5-MeITP	260 ± 98	0.042 ± 0.008	$1.62 * 10^2$	11 %
5-EtITP	184 ± 36	0.079 ± 0.007	$4.3 * 10^2$	29 %
5-EyITP	41.3 ± 9.2	0.030 ± 0.002	$7.14 * 10^2$	48 %
4-NITP	28 ± 10	0.052± 0.004	$1.84 * 10^3$	122 %
6- NITP	53 ± 13	0.097 ± 0.008	$1.82 * 10^3$	122 %
5-NITP	264 ± 31	0.036 ± 0.002	$1.34 * 10^2$	9%

Objective 2: Biological testing of non-natural nucleosides against lung cancer cell lines.

Task 2A. To evaluate the function of non-natural nucleosides as anti-cancer agents. We have measured the dose-dependency of the corresponding non-natural deoxyribosides developed under Objective 1. Specifically, IC_{50} and LD_{50} values are being measured against the following cell lines: A549, ACC-LC-48, AA8pIK8, and H69AR. Cell viability and growth are assessed via routine MTT assays using a microplate reader. Figure 7 provides a representative dose response curve for the anti-cancer effects of one of our non-natural nucleosides, 5-NIdR, against the A549 cell line. Note that we tested this specific analog first as we previously demonstrated using leukemia cells (MOLT4 and CEM-C7) as well as adherent cells (HCT116 (colon), U87 (glioblastoma), and fibroblasts) that 5-NIdR displays low potency when used as a monotherapeutic agent. The data presented here recapitulates this result. However, 5-NIdR works synergistically with certain DNA damaging agents such as temozolomide which produces non-instructional lesions such as abasic sites. We are currently testing the ability of 5-NIdR and other modified nucleoside analogs to work in combination with therapeutic agents which create reactive oxygen species and that are likely to generate DNA lesions such as 8-oxoguanine. In addition, we are assessing cell viability and cell growth via microscopy studies (data not shown). We anticipate this Task to be completed with six (6) months.

Figure 7. Dose response curve for the anti-cancer effects of 5-NIdR against the lung cancer cell line, A549.

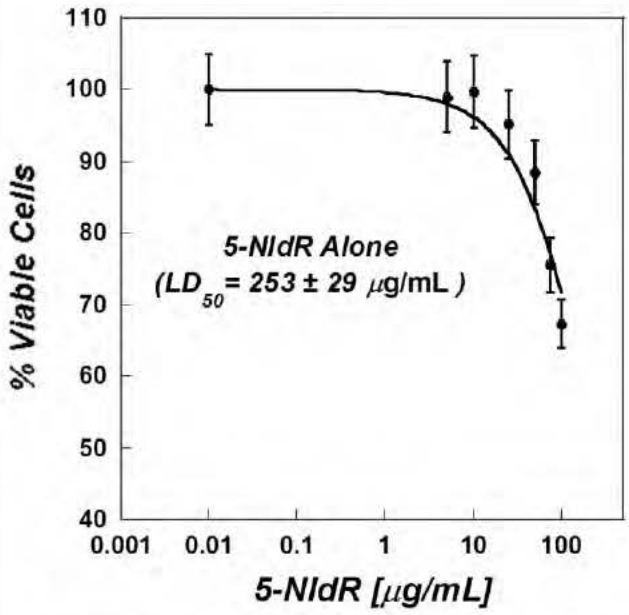

Task 2B. To Evaluate the Mechanism of Cell Death. Flow-cytometry studies are planned over the next six (6) months to investigate the mechanism of cell death induced by the corresponding non-natural nucleoside analogs. The primary technique is propidium iodide and annexin V staining to differentiate between apoptosis versus necrosis. Figure 8 provides representative plots from dual parameter flow cytometry experiments examining the anti-cancer effects of 5-NIdR against the A549 cell line. These data demonstrate that treatment with 100 mg/mL of 5-NIdR alone does produce a significant increase in apoptosis compared to cells treated with DMSO (vehicle control). We expect to observe a synergistic increase in apoptosis in cells treated with

Figure 8. Dual parameter flow cytometry measuring the anti-cancer effects of DMSO versus 5-NIdR against the A549 cell line.

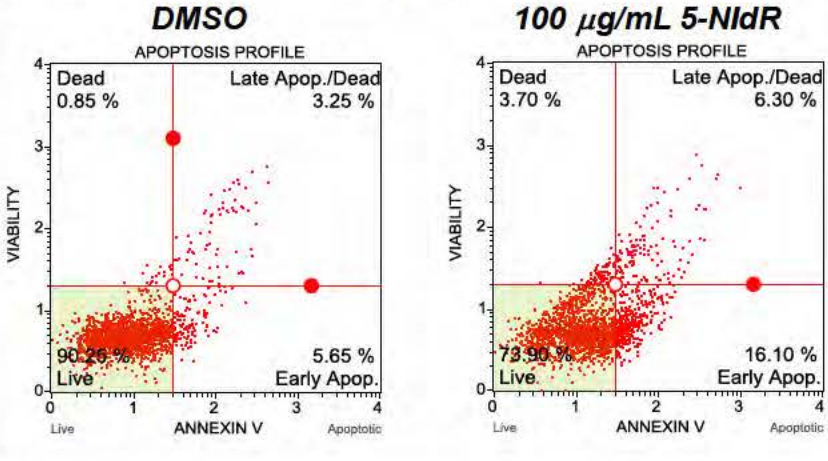

a combination of 5-NIdR and reactive oxygen species designed to generate 8-oxoguanine. Other biochemical analyses including caspase activation, PARP cleavage, and DNA fragmentation patterns will be performed to validate apoptotic cell death. We anticipate this Task to be completed with six (6) months.

Task 2C. siRNA Knockdown Experiments to Identify Specialized DNA Polymerases Involved in Utilizing Non-Natural Nucleosides. siRNA knockdown experiments will be performed targeting various specialized DNA polymerase such as polymerase eta, iota, and kappa that are involved in replicating damaged DNA. Our kinetic data obtained under Task 1B indicates that pol eta may be the primary polymerase responsible for misreplcating oxidized DNA lesions such as 8-oxoguanine. We have purchased siRNA to knockdown the levels of pol eta expression in lung cancer cell lines including A549, ACC-LC-48, AA8pIK8, and H69AR. However, we are awaiting the results of studies examining the dose-dependency of the corresponding non-natural deoxyribosides before embarking on these studies.

Objective 3: Validating the diagnostic applications of therapeutic nucleoside analogs.

Task 3A. *In vitro* validation assays. *In vitro* "clicking" reactions were performed using our published protocols to verify that the non-natural nucleotides could function as effective diagnostic probes to detect the replication of damaged DNA. As expected, all of the non-natural nucleotides developed here function as diagnostic probes. However, there are some differences in the overall efficiencies for the “clicking” reactions that range from 45-75% efficiency. We are exploring the mechanistic reason for these differences to better optimize this capability. Regardless, we anticipate that these variations will not complicate the completion of our cell based studies.

Task 3B. Validation of Diagnostic Applications by Cell-Based Studies. In situ "clicking" reactions are planned using the nucleoside analogs developed in Objective 1. These studies have been delayed due to time issues with the synthesis and testing of the new lead compounds described in **Task 1A** and **1B**. We anticipate this Task to be completed within the next twelve (12) months.

4. Key Research Accomplishments:

- ❖ Completed the synthesis and chemical characterization of six (6) distinct nucleotide analogs.
- ❖ Measured the incorporation of sixteen (16) distinct nucleotide analogs opposite 8-oxo-guanine, a miscoding DNA lesion associated with lung cancer.
- ❖ Identified two (2) nucleotide analogs that are efficiently and selectively incorporated opposite 8-oxo-guanine.
- ❖ Demonstrated that one nucleotide analog functions as a chain-terminating substrate for pol eta.
- ❖ Tested the biological activity of these analogs against several lung cell lines including A549, ACC-LC-48, AA8pIK8, and H69AR.
- ❖ Submitted a manuscript entitled "A comparative study of DNA polymerase activity during translesion DNA synthesis: The use of modified and non-natural nucleotides provide unique insights into pro-mutagenic replication." to Nucleic Acid Research.

5. Conclusion:

More people in the United States die from lung cancer than any other type of cancer. The development and progression of lung cancer is in most cases directly linked to mutagenesis caused by the misreplication of damaged DNA. Our research funded by the Department of Defense has provided new insight into this process. In this respect, we have identified several novel nucleotide analogs that function as effective DNA polymerase substrates when replicating DNA lesions associated with lung cancer. These analogs have provided a deeper understanding of the molecular mechanisms for lung cancer development as well as acquired resistance to treatment with DNA damaging agents. Perhaps more importantly, these analogs are being used to develop an innovative strategy for treating early stage lung cancer. Finally, our studies are applying these analogs as predictive and prognostic markers to identify non-responders of chemotherapeutic agents that cause DNA damage.

6. Publications, Abstracts, and Presentations:

Publication: "A comparative study of DNA polymerase activity during translesion DNA synthesis: The use of modified and non-natural nucleotides provide unique insights into pro-mutagenic replication." Submitted to Nucleic Acid Research.

7. Inventions, Patents, and Licenses: None to date

8. Reportable Outcomes: None to date

9. Other Achievements: None to date

10. References: ***N/A***

11. Appendices: See attached manuscript

A comparative study of DNA polymerase activity during translesion DNA synthesis: The use of modified and non-natural nucleotides provide unique insights into pro-mutagenic replication

Jung-Suk Choi[1], Anvesh Dasari[1], Peter Hsu[2], Stephen J. Benkovic[2], and Anthony J. Berdis[1,3,#]

[1]Department of Chemistry and [3]the Center for Gene Regulation in Health and Disease, Cleveland State University, 2351 Euclid Avenue, Cleveland, OH 44115, USA

[2] Department of Chemistry, The Pennsylvania State University, 413 Wartik Building, University Park, PA 16802, USA

#Corresponding Author Information: Tel (216) 687-2454, Fax (216) 687-9298,

e-mail: a.berdis@csuohio.edu

Keywords: Mutagenesis, DNA polymerases, oxidative stress, translesion DNA synthesis, nucleoside analogs

Abbreviations and Textual Footnotes

[1] Abbreviations include the following: EDTA, Ethylenediaminetetraacetic acid; dNTP, deoxynucleoside triphosphate; TLS, translesion DNA synthesis; ROS, reactive oxygen species; 8-oxo-G, 8-oxoguanine; FaPyG, 2,6-diamino-4-oxo-5-formamidopyrimidine; A, adenine; C, cytidine; G, guanine; T, thymine; dAMP, adenosine-2'-deoxyriboside monophosphate; dCMP, cytosine-2'-deoxyriboside monophosphate; dATP, adenosine-2'-deoxyriboside triphosphate; dGTP, guanosine-2'-deoxyriboside triphosphate; N^6-MedATP, N^6-methyl-adenosine-2'-

deoxyriboside triphosphate; 6-Cl-dATP, 6-chloropurine-2’-deoxyadenosine-5’-triphosphate; 6-Cl-2APTP, 6-chloro-2-amino-2’-deoxyriboside-5’-triphosphate; O^6-MedGTP, O^6-methylguanosine-2’-deoxyriboside triphosphate; N^2-MedGTP, N^2-methyl-guanosine-2’-deoxyriboside triphosphate; 2-6-dATP, 2,6-diaminopurine-2’-deoxyriboside-5’-triphosphate; dITP, 2'-deoxyinosine-5’-triphosphate; 8-oxo-dGTP, 8-oxoguanine-5’-triphosphate; IndTP, indolyl-2’-deoxyriboside triphosphate; 5-MeITP, 5-methy-lindolyl-2’-deoxyriboside triphosphate; 5-Et-ITP, 5-ethyl-indolyl-2’-deoxyriboside triphosphate; 5-EyITP, 5-ethylene-indolyl-2’-deoxyriboside triphosphate; 5-NITP, 5-nitro-indolyl-2’-deoxyriboside triphosphate; 4-NITP, 4-nitro-indolyl-2’-deoxyriboside triphosphate; 6-NITP, 6-nitro-indolyl-2’-deoxyriboside triphosphate.

Abstract. Oxygen-rich environments can create pro-mutagenic DNA lesions such as 8-oxoguanine (8-oxo-G) that can be misreplicated during **t**rans**l**esion DNA **s**ynthesis (TLS). This report evaluates the pro-mutagenic behavior of 8-oxo-G by quantifying the ability of high-fidelity and specialized DNA polymerases to incorporate natural and modified nucleotides opposite this lesion. Although high-fidelity DNA polymerases (eukaryotic pol δ and bacteriophage T4 DNA polymerase) display error-prone tendencies when replicating 8-oxo-G, they display remarkably low efficiencies for TLS compared to normal DNA synthesis. In contrast, pol η shows a combination of high efficiency and low fidelity when replicating 8-oxo-G. These combined properties are consistent with a pro-mutagenic role for pol η when replicating this DNA lesion under cellular conditions. Kinetic studies with modified nucleotide analogs indicate that pol η relies heavily on hydrogen-bonding interactions during normal and translesion synthesis. However, some nucleobase modifications including alkylation to the O^6 and N^2 position of guanine increase error-prone replication of 8-oxo-G. A model is proposed for enhanced pro-mutagenic replication caused by reactive oxygen species that couples efficient incorporation of damaged nucleotides opposite oxidized DNA lesions. The biological implications of this model toward increasing mutagenic events are discussed in the context of diseases such as lung cancer.

DNA replication is the biological process in which an organism's genome is copied by the action of at least one DNA polymerase. The vast majority of DNA polymerases use the coding information present on the templating strand of DNA (or RNA) to guide each nucleotide incorporation event. The efficiency and fidelity of this process are often attributed to the formation of complementary hydrogen-bonding interactions that define a correct base pair (1,2). In this regard, DNA polymerization is analogous to reading a simple binary code in which the mutual recognition of adenine (A) by thymine (T) and of guanine (G) by cytosine (C) involves complementarity in shape, size, and hydrogen-bonding interactions made between each base pair. Using these interactions, most replicative DNA polymerases synthesize DNA with an incredible degree of fidelity, making only 1 mistake every million opportunities (3). It is even more impressive that many DNA polymerases maintain this high degree of accuracy while synthesizing DNA at remarkably high speeds of >500 base pairs/second (4).

While the molecular mechanism of normal DNA synthesis is well understood, the underlying processes by which DNA polymerases replicate damaged DNA are less defined. Much of this deficiency arises from two major complications that include the diversity of DNA lesions formed inside the cell and the number of DNA polymerases that can replicate each lesion. For example, there are over a hundred different DNA lesions that can form within a cell (5), and many of these lesions can drastically influence DNA polymerase activity (6). For instance, commonly formed lesions such as abasic sites and thymine dimers can distort the proper conformation of the DNA template to significantly hinder the kinetics of nucleotide incorporation catalyzed by high-fidelity DNA polymerases (7-9). In fact, these particular DNA lesions are considered to be strong replication blocks for most high-fidelity DNA polymerases due to their ability to inhibit DNA synthesis. Inside the cell, the constant interruption of DNA

synthesis catalyzed by high-fidelity DNA polymerases would wreak havoc on the continuity of DNA replication and produce devastating effects on cell viability and proliferation. In order to avoid catastrophic failures associated with replicating damaged DNA, prokaryotic and eukaryotic cells possess different "specialized" DNA polymerases that can efficiently replicate these lesions. The ability to by-pass damaged DNA, a process termed translesion DNA synthesis (TLS), can result in “error-free” or “error-prone” replication. While “error-prone” activity during TLS may reduce genomic fidelity, it is essential as most cells would die without specialized DNA polymerases that efficiently replicate non-instructional DNA lesions such as abasic sites.

However, not all forms of DNA damage produce such dire consequences on DNA synthesis. In fact, most DNA lesions contain subtle modifications that simply alter the hydrogen-bonding potential of the nucleobase rather than cause major distortions to the DNA template. These simple modifications can enhance the extent of pro-mutagenic replication by increasing the frequency of misincorporation events catalyzed by DNA polymerases (10-12). Increased mutagenic DNA synthesis is a hallmark of several hyperproliferative diseases, most notably cancer. Lung cancer represents an important example as the oxygen-rich environment of the lung can produce reactive oxygen species (ROS) that can generate several pro-mutagenic DNA lesions such as 2,6-diamino-4-hydroxy-5-formamidopyrimidine (faPyG) and 8-oxo-guanine (8-oxo-G) (Figure 1A). Both lesions are considered to be miscoding as they can be replicated in an “error-free” or “error-prone” manner (13, 14). For example, 8-oxo-G can be replicated incorrectly via the incorporation of dAMP, leading to an overall increase in G:C to T:A transversion mutations. At the molecular level, the misreplication of 8-oxo-G depends upon the *syn*- versus *anti*-conformation of the oxidized nucleobase. As illustrated in Figure 1B, “error-free” DNA synthesis occurs via dCMP insertion opposite 8-oxo-G which is favored when the

oxidized nucleobase is in the *anti*-conformation and identical to an unmodified guanine. In contrast, pro-mutagenic synthesis, i.e., dAMP insertion opposite 8-oxo-G, is favored when the oxidized nucleobase is in the *syn*-conformation and resembles thymine.

As indicated earlier, the second complication for precisely defining the mutagenic potential of a DNA lesion such as 8-oxo-G is the number of DNA polymerases that are involved in its cellular replication. This is especially complex in human cells as they possess 15 different DNA polymerases that can be classified based on their biological function (15). One group includes "high-fidelity" polymerases such as pol δ, pol ε, and pol γ that are primarily involved in chromosomal and mitochondrial DNA synthesis. Another group includes pol η, pol ι, pol θ, pol ζ, pol κ, and the Rev1 protein that were originally termed "error-prone polymerases" due to their remarkable lack of fidelity when replicating undamaged DNA (16-18). For example, pol η displays a high error frequency of 1 mistake every 100 to 1,000 opportunities when replicating undamaged DNA (16, 17). However, several groups have demonstrated that pol η can effectively and accurately replicate crosslinked DNA lesions such as thymine dimers and cisplatinated DNA (19-21). A third group of DNA polymerases include pol β, pol λ, pol μ, and terminal deoxynucleotidyl transferase (TdT) which are typically involved in DNA repair pathways. Many of these DNA polymerases display variable fidelity depending upon the nature of the DNA substrate (normal or damaged DNA) used during replication. This brief overview again highlights the difficulty in defining the mutagenic potential of a DNA lesion due to the large number of DNA polymerases that can replicate damaged DNA.

To develop a more comprehensive understanding of TLS and mutagenesis, we quantified the abilities of high-fidelity and specialized DNA polymerases to replicate the miscoding lesion, 8-oxo-G. Our kinetic analyses demonstrate that the overall efficiency of high-fidelity DNA

polymerases is reduced ~1,000-fold when replicating 8-oxo-G. This reduction in efficiency suggests that these polymerases are unlikely to replicate this miscoding lesion under physiological conditions. Consistent with this model, the specialized DNA polymerase, pol η, performs TLS ~100-fold more efficiently than either high-fidelity DNA polymerase. In addition, pol η misinserts dAMP opposite 8-oxo-G with a high efficiency that is comparable to dCMP insertion. The combination of high efficiency and promiscuity for misinserting dAMP likely contributes to the mutagenic potential of the oxidized DNA lesion. At the molecular level, we further demonstrate that pol η relies heavily of the presence of hydrogen bonding functional groups to efficiently replicate normal and damaged DNA. This is evident as most modifications to the hydrogen bonding groups on the incoming dNTP reduce the efficiency of nucleotide utilization. However, one specific nucleotide, N^2-MedGTP, shows an increase in utilization and selectivity for TLS activity catalyzed by pol η. This result suggests that inappropriate modifications to DNA and nucleotide pools can cause a synergistic increase in pro-mutagenic DNA synthesis. The biological ramifications of these findings are discussed in the context of disease models such as lung cancer in which increased levels of reactive oxygen species can enhance disease development and progression.

MATERIALS AND METHODS

Materials. [$\gamma -^{32}$P]-ATP was purchased from MP Biomedical (Irvine, CA). Unlabelled dNTPs (ultrapure) were obtained from Pharmacia. Unlabeled dNTPs (ultrapure) were obtained from Pharmacia. Magnesium acetate, magnesium chloride, and Trizma base were from Sigma. Urea, acrylamide, and bis-acrylamide were from National Diagnostics (Rochester, NY). Oligonucleotides, including those containing 8-oxo-guanine, were synthesized by Operon Technologies (Alameda, CA). All modified nucleotides including N^6-MedATP, 6-Cl-PTP, 6-Cl-2APTP, O^6-MedGTP, N2-MedGTP, 2-6-dATP, dITP, and 8-oxo-dGTP were obtained from Trilink Biotechnologies (San Diego, CA). All non-natural nucleotides including IndTP, 5-MeITP, 5-Et-ITP, 5-EyITP, 5-NITP, 4-NITP, and 6-NITP were synthesized and purified as previously reported (22-25). All other materials were obtained from commercial sources and were of the highest available quality. Exonuclease-deficient bacteriophage T4 DNA polymerase (gp43exo$^-$ (Asp-219 to Ala mutation)) was purified and quantified as previously described (26). Polymerase delta and polmerase eta were purified as previously described (27, 28).

Kinetic parameters for nucleotide incorporation. Kinetic studies using the bacteriophage T4 DNA were performed using an assay buffer consisting of TrisOAc (25 mM pH 7.5), KOAc (150 mM), DTT (10 mM), and 10 mM MgAcetate at pH 7.5. Kinetic studies using polymerase delta and eta were performed using an assay buffer consisting of TrisOAc (50 mM pH 7.5), bovine serum albumin (1 mg/mL), DTT (10 mM), and 5 mM $MgCl_2$ at pH 7.5. All assays were performed at 25 °C unless otherwise noted. The kinetic parameters (k_{cat}, K_m, and k_{cat}/K_m) for nucleotides were measured as previously described (29). Briefly, a typical assay was performed by pre-incubating DNA substrate (500 nM) with a limiting amount of polymerase (10 or 25 nM) in assay buffer and Mg^{2+}. Reactions were initiated by adding variable concentrations of

nucleotide substrate (1–500 μM). At variable time intervals, 5 μL aliquots of the reaction were quenched by adding an equal volume of 200 mM EDTA. Polymerization reactions were monitored by analyzing products on 20% sequencing gels as previously described (29). Gel images were obtained with a Packard PhosphorImager by using the OptiQuant software supplied by the manufacturer. Product formation was quantified by measuring the ratio of ^{32}P-labeled extended and un-extended primer. The ratios of product formation are corrected for substrate in the absence of polymerase (zero point). Corrected ratios are then multiplied by the concentration of primer/template used in each assay to yield total product. Steady-state rates were obtained from the linear portion of the time course and were fit to Equation 1

$$y = mx + b \quad (1)$$

where m is the slope of the line corresponding to the rate of the polymerization reaction (nM s^{-1}), b is the y-intercept, and t is time. Data for the dependency of rate as a function of nucleotide concentration were fit to the Michaelis–Menten equation (Equation 2):

$$v = V_{max} * [dNTP] / (K_m + [dNTP]) \quad (2)$$

where v is the rate of product formation (nM s^{-1}), V_{max} is the maximal rate of polymerization, K_m is the Michaelis constant for dXTP, and [dXTP] is the concentration of nucleotide substrate. The turnover number, k_{cat}, is V_{max} divided by the final concentration of polymerase used in the experiment.

RESULTS

Comparing Normal versus Translesion DNA Synthesis Activity between High-Fidelity and Specialized DNA Polymerases. This study begins by comparing the ability of two high fidelity DNA polymerases (bacteriophage T4 DNA polymerase (gp43 exo$^-$) and eukaryotic pol δ) and a specialized DNA polymerase (pol η) to incorporate natural dNTPs opposite normal and damaged nucleobases. Defined DNA substrates containing G, C, or 8-oxo-G at position 14 of the template (Figure 2A) were used to accurately quantify the activity of each DNA polymerase. Denaturing gel electrophoresis images provided in Figure 2B illustrate the ability of these DNA polymerases to perform normal (dCMP insertion opposite G), incorrect (dAMP insertion opposite G) and translesion DNA synthesis (dCMP or dAMP insertion opposite 8-oxo-G). During normal DNA synthesis, both high-fidelity polymerases are remarkably faithful as they insert dCMP opposite G much more efficiently than dAMP. However, gp43 exo$^-$ and pol δ exhibit pro-mutagenic tendencies during TLS by efficiently incorporating dAMP opposite 8-oxo-G. In contrast, the specialized polymerase, pol η, displays less fidelity when replicating undamaged DNA, and this result that is consistent with previous reports (16-18). Although pol η inserts dAMP opposite G, dCMP is preferentially incorporated opposite undamaged DNA. However, pol η displays more promiscuous behavior when replicating 8-oxo-G as dATP and dCTP are utilized with nearly equal efficiencies. As such, these data suggest that pol η catalyzes pro-mutagenic DNA synthesis more effectively than either high fidelity DNA polymerase.

To more accurately assess the kinetic behavior of these polymerases, k_{cat}, K_m, and k_{cat}/K_m values were measured for dCTP and dATP opposite G and 8-oxo-G. Michaelis-Menten plots for dCMP incorporation opposite G (left panel) or 8-oxo-G (right panel) catalyzed by gp43 exo$^-$ are provided in Figure 2C. The kinetic parameters for the bacteriophage T4 DNA polymerase during

normal and translesion DNA synthesis are summarized in Table 1. As expected, gp43 exo$^-$ shows a high catalytic efficiency for normal DNA synthesis of 1.7 *10^5 $M^{-1}sec^{-1}$ that is achieved by a relatively low K_m value of 4.7 μM for dCTP and a fast k_{cat} value of 0.94 sec^{-1}. When replicating 8-oxo-G, however, the catalytic efficiency of gp43 exo$^-$ decreases by ~20-fold in which the K_m value for dCTP increases 10-fold (K_m = 54 μM) while the k_{cat} value is reduced 2-fold (k_{cat} = 0.59 sec^{-1}). Surprisingly, the efficiency for inserting dAMP opposite 8-oxo-G is only 4-fold lower than dCMP (compare k_{cat}/K_m values of 11,000 $M^{-1}sec^{-1}$ for dCTP versus 3,000 $M^{-1}sec^{-1}$ for dATP). This decrease in catalytic efficiency is caused exclusively by a large increase in the K_m value for dATP (compare K_m values of 54 μM versus 250 μM for dCTP and dATP, respectively).

Identical experiments were performed using pol δ, the high-fidelity eukaryotic DNA polymerase, and representative Michaelis-Menten plots are provided in Figure 2D. The kinetic parameters for pol δ during normal and translesion DNA synthesis are summarized in Table 1. These data indicate that pol δ is also highly proficient at replicating undamaged G, displaying a low K_m of 0.64 μM for dCTP and a fast k_{cat} of 1 sec^{-1}. Similar to the bacteriophage T4 polymerase, the efficiency of replicating 8-oxo-G is greatly reduced as both the K_m for dCTP and k_{cat} are significantly worse. In particular, the K_m value of 34 μM measured for dCTP during TLS is 50-fold higher than that for normal DNA synthesis. Likewise, the k_{cat} for pol δ is reduced ~30-fold when replicating the oxidized lesion. This later result indicates that the rate-limiting step for polymerase turnover is sensitive to the nature of the DNA lesion and represents an interesting difference between pol δ and gp43exo- toward replicating 8-oxo-G.

The kinetic parameters for the specialized DNA polymerase, pol η, are considerably different than either high-fidelity DNA polymerase. As illustrated in Figure 2E, the Michaelis-

Menten plots for inserting dCMP opposite G or 8-oxo-G are remarkably similar. Indeed, the K_m values for dCTP are nearly identical (compare 1.3 μM versus 3.0 μM for G and 8-oxo-G, respectively). Furthermore, the k_{cat} value during TLS is only 2-fold lower than that for replicating normal DNA (compare 0.40 sec^{-1} versus 0.88 sec^{-1} for 8-oxo-G and G, respectively). Collectively, these data demonstrate that pol η misinserts dAMP opposite 8-oxo-G with a high overall high catalytic efficiency of 24,000 $M^{-1}sec^{-1}$. In fact, the catalytic efficiency for pol η misinserting dAMP opposite the oxidized lesion is 60-fold higher than that measured for pol δ. The higher efficiency suggests that pol η is more proficient at catalyzing "error-prone" replication of 8-oxo-G compared to pol δ. The kinetic parameters for pol η during normal replication and TLS are summarized in Table 1.

Quantifying the Incorporation of Modified Nucleotide Analogs by Pol η. Several models have been proposed to explain the low replicative fidelity displayed by pol η (30-33). One invokes the contributions of hydrogen-bonding interactions made between the incoming nucleotide with the templating nucleobase and/or amino acids that reside within the polymerase's active site. An alternative model suggests that pol η possesses a "loose" active site that is large enough to accommodate bulky DNA lesions. The "loose" active site architecture of pol η differs from the "tight" active site of most high-fidelity DNA polymerases (34) which generally do not accommodate most bulky lesions.

To further investigate these mechanisms, we quantified the incorporation of purine nucleoside triphosphates containing alterations to hydrogen-bonding functional groups (Figure 3A). These modified nucleotides are classified into three distinct groups. The first includes alkylated nucleotides such as N^6-MedGTP, O^6-MedGTP, and N^2-MedGTP that were used to evaluate the collective contributions of hydrogen-bonding, shape complementarity/steric fit, and

nucleobase hydrophobicity on nucleotide utilization. The second group are analogs in which a hydrogen-bonding group is replaced with a halogen (6-Cl-dATP and 6-Cl-2APTP). These substitutions provide a way to more accurately evaluate the contributions of shape complementarity/steric fit and nucleobase hydrophobicity. The final group are purines in which hydrogen-bonding groups are removed (dITP) or added (2,6-dATP). These analogs were used to interrogate the contributions of hydrogen-bonding interactions during normal versus translesion DNA synthesis.

The kinetic parameters, k_{cat}, K_m, and k_{cat}/K_m, for these analogs were first measured for incorporation opposite 8-oxo-G. Figure 3B provides representative Michaelis-Menten plots comparing the utilization of dATP versus 6-Cl-PTP during the replication of 8-oxo-G. These data demonstrate that replacing a hydrogen-bonding group ($-NH_2$) with a halogen (non-hydrogen bonding group) lowers the overall catalytic efficiency by producing negative effects on both K_m and k_{cat}. In particular, the reduced efficiency for utilizing 6-Cl-PTP compared to dATP is caused by a 3-fold increase in K_m coupled with a 3-fold decrease in k_{cat}. Table 2 provides a summary of kinetic parameters for other modified nucleotide analogs. In most cases, modification to one or more hydrogen-bonding groups present on the incoming nucleotide causes a reduction in incorporation efficiencies. For example, both 6-Cl-PTP and 6-Cl-2APTP have lower efficiencies for insertion opposite 8-oxo-G, and these results again indicate that hydrogen bonding groups are important for optimal polymerization catalyzed by pol η. However, the position of the hydrogen bonding group also appears critical for nucleotide utilization as well. This is evident as analogs such as 2,6-dATP and ITP have lower incorporation efficiencies compared to dATP. In fact, 8-oxo-dGTP represents the worst substrate tested for insertion opposite 8-oxo-G as the catalytic

efficiency is 50-fold lower than dATP and 16-fold lower than dGTP. This reduction is likely caused by alterations in the *anti*- versus *syn*-conformation of the nucleotide (35).

It should be noted that some modifications to a hydrogen-bonding group produce a minimal effect on nucleotide utilization. For example, the efficiency for O^6-MedGTP is only 2-fold lower than dATP while that for N^6-MedATP is slightly higher than dATP. However, there is one remarkable instance in which alkylation of a hydrogen-bonding group engenders a significant positive effect on nucleotide incorporation opposite damaged DNA (Figure 3C). In this case, N^2-MedGTP is utilized ~10- and 20-fold fold more effectively than dATP and dGTP, respectively. The increased utilization of N^2-MedGTP occurs via a large enhancement in its K_m value rather than through an effect on k_{cat}. This represents an unusual case as the apparent binding affinities for most modified nucleotides remain either unchanged or become worse compared to dATP. In fact, the K_m value for the majority of analogs remains fairly constant at ~50 μM while the k_{cat} value is the kinetic parameter that varies more significantly amongst these modified analogs. With the exception of N^2-MedGTP, the collective data set suggest that the binding of an incoming nucleotide is not significant influenced by hydrogen-bonding interactions. Instead, k_{cat} values appear highly sensitive to both the number and orientation of hydrogen-bonding groups.

To verify that this conclusion is not only valid during TLS, we quantified the effects of these modifications on the efficiency of replicating undamaged DNA. Representative denaturing gel electrophoresis images provided in Figure 3D compare the incorporation of these modified nucleotides opposite G versus 8-oxo-G. These results illustrate that most modified nucleotides are preferentially incorporated opposite 8-oxo-G versus G. This conclusion was verified by examining the kinetic parameters for their incorporation opposite G. As summarized in Table 2,

the catalytic efficiencies for most modified analogs are 10- to 100-fold lower during normal synthesis compared to TLS. In most cases, these reductions are caused by adverse effects on k_{cat} rather than through perturbations in the K_m value for a modified analog. Again, these data support a model in which nucleotide binding is relatively independent of the presence (or absence) of hydrogen-bonding groups. Instead, the k_{cat} value is more sensitive to the presence (or absence) of hydrogen-bonding groups.

Collectively, these kinetic data indicate that modifications to a natural dNTP lead to an enhancement in "error-prone" replication of 8-oxo-G but not of an unmodified guanine. This observation is significant for several reasons. First, this result indicates that the intrinsic fidelity of pol η is not unilaterally affected by modifications to an incoming dNTP. Instead, these modifications selectively decrease fidelity during the replication of damaged DNA. N^2-MedGTP represents the best example of this phenomenon as this modified nucleotide shows a ~40-fold higher selectivity for insertion opposite 8-oxo-G than G (Figure 3C). The greater selectivity of N^2-MedGTP for damaged DNA coupled with its 10-fold higher catalytic efficiency highlights a pro-mutagenic role for pol η during the replication of damaged DNA.

Incorporation of 5-Substituted Indolyl Nucleotide Analogs by Pol η. To further evaluate the role of hydrogen-bonding, shape complementarity, and hydrophobicity, we next quantified the incorporation of the 5-substituted indolyl-2'-deoxynucleotide analogs depicted in Figure 4A. Representative denaturing gel electrophoresis data provided in Figure 4B demonstrate that these non-natural nucleotides behave as poor substrates for pol η during both normal and translesion DNA synthesis. This result again highlights how removing canonical hydrogen bonding functional groups produces a negative effect on nucleotide utilization by pol η. As summarized in Table 3, the catalytic efficiencies for these non-natural nucleotides are between 5- to 1,000-

fold lower than dATP. This decrease efficiency is caused primarily by reductions in k_{cat} rather than through significant perturbations in K_m. The effect on k_{cat} values reiterate that the rate-limiting step for pol η turnover is highly sensitive to proper hydrogen bonding interactions. While these data suggest that hydrogen-bonding interactions are important for the polymerization cycle, they also suggest steric-fit plays an important role as well. This is evident as the overall size of the incoming nucleotide influences the catalytic efficiency for nucleotide insertion. For instance the k_{cat}/K_m for 5-MeITP, a good pairing partner for the *syn*-conformation of 8-oxo-G, is 3-fold higher than that measured for the smaller analog, IndTP (Figure 3C). Similarly, the k_{cat}/K_m decreases as the size of the incoming nucleotide increases beyond the optimal interglycosyl basepair distance of 10.6Å for a normal Watson-Crick base pair. In particular, the k_{cat}/K_m for 5-EtITP is 10-fold lower than that for 5-MeITP. Despite being similar in shape in size, 5-EyITP is utilized 10-fold less efficiently than 5-EtITP. This result suggests that entropic effects can also influence nucleotide utilization by pol η. In this case, the conjugated double bond reduces rotational freedom of the functional group, and this entropic penalty could diminish the utilization of 5-EyITP as a substrate. Consistent with this model, 5-NITP displays the highest catalytic efficiency amongst all 5-substituted indolyl-nucleotides tested here. We argue that the rotational freedom of the nitro group can increase its incorporation efficiency. However, other features such as increased pi-stacking interactions present in the nitro moiety may also play a role as this was previously demonstrated for high-fidelity DNA polymerases when replicating non-instructional DNA lesions (36, 37).

The Position of the Nitro Moiety Influences the Efficiency and Selectivity for Incorporation. We previously demonstrated that the position of the nitro moiety can significantly affect the selectivity of different high-fidelity DNA polymerases during the replication of normal and

damaged DNA (25). Here, we tested if pol η behaves similarly and shows a preference for utilizing one of these nitro-containing nucleotides during normal or translesion DNA synthesis.

During the replication of 8-oxo-G, pol η utilizes 4-NITP with an identical catalytic efficiency compared to 5-NITP. However, the K_m for 4-NITP is ~2.5-fold lower than 5-NITP while the k_{cat} for 4-NITP is 2.5-fold lower than 5NITP. Surprisingly, 6-NITP is a very efficient substrate for pol η as the k_{cat}/K_m for 6-NITP is 13-fold higher than either 4-NITP or 5-NITP. Furthermore, the efficiency for 6-NITP is 3-fold greater than the preferred natural substrate, dATP. The higher catalytic efficiency for 6-NITP is caused by a 15-fold decrease in its K_m values while the k_{cat} value remains identical to that measured for 5-NITP. While 6-NITP is highly efficient for insertion opposite 8-oxo-G, it displays only a slight preference (2-fold) for 8-oxo-G compared to G. A more interesting dichotomy is observed for the selectivity of 4-NITP. In this case, 4-NITP is poorly utilized by pol η during the replication of G. As such, 4-NITP displays a ~10-fold higher selectivity for incorporation opposite the oxidized lesion versus G. Collectively, these data demonstrate that the efficiency and selectivity of substrate utilization can both be influenced by permutations in the position of the nitro moiety.

Discussion

Mutagenesis, the inappropriate change in an organism's genomic information, is a complex biological process that is influenced by numerous factors. These include the type of DNA damage inflicted on the cell, the various DNA repair pathways that can process the formed lesions, and the activity of DNA polymerases that can incorporate nucleotides opposite unrepaired DNA lesions. Another level of complexity is the number and diversity of DNA lesions that can form after exposure to DNA damaging agents. For example, hyperoxic conditions present in organs such as the lung can generate reactive oxygen species (ROS) which in turn can produce several oxidized DNA lesions. The misreplication of these lesions can significantly increase the risk of cancer cancer. To better understand how the misreplication of damaged DNA can influence cancer initiation, we compared the ability of high-fidelity and specialized DNA polymerases to replicate 8-oxo-G, a lesion commonly formed by ROS. Our results validate that 8-oxo-G is a pro-mutagenic DNA lesion as each DNA polymerase tested here incorporate dCMP and dAMP opposite this oxidized base, resulting in either "error-free" and "error-prone" replication, respectively. Indeed, both high-fidelity DNA polymerases display "error-prone" tendencies as their efficiencies for inserting dCMP opposite 8-oxo-G are only 5-fold higher than those measured for inserting dAMP. This reduced fidelity contrasts that for the normal replication of G in which the efficiency for dCMP incorporation is 10^6-fold higher than dAMP misincorporation. At face value, the reduced fidelity replicating 8-oxo-G suggests that high fidelity polymerases are responsible for the cellular misreplication of this oxidized lesion. However, we argue that this is unlikely for several reasons. Most notably, the catalytic efficiencies for utilizing dCTP or dATP are remarkably low, especially when compared to normal DNA synthesis. In particular, the k_{cat}/K_m values measured for inserting dCMP opposite 8-

oxo-G are orders of magnitude lower than inserting dCMP opposite G. The reduced efficiency for replicating the oxidized base is not surprising as changes to the hydrogen-bonding potential of a templating nucleobase often produce adverse effects on the kinetics of DNA polymerization. For example, we previously demonstrated that the catalytic efficiency displayed by the bacteriophage T4 DNA polymerase for inserting dAMP opposite an abasic site, a non-instructional DNA lesion, is 1,000-fold lower than incorporating dATP opposite T (29). Similar results have been observed with the eukaryotic DNA polymerase, pol δ (8, unpublished results, AJB).

In contrast, the specialized DNA polymerase, pol η, is relatively efficient at inserting both dCMP and dAMP opposite 8-oxo-G. In fact, the catalytic efficiencies for each nucleotide are nearly identical, and this equality predicts an overall high frequency for pol η to misreplicate 8-oxo-G compared to pol δ which preferentially incorporates dCTP. Furthermore, pol η displays a higher overall catalytic efficiency for replicating the lesion compared to high fidelity DNA polymerases. We argue that the difference in replication efficiency between high-fidelity and specialized polymerases is consistent a model in which pol η is the primary polymerase involved in replicating 8-oxo-G in an "error-prone" manner (Figure 5). In this model, the high fidelity DNA polymerase, pol δ, would first encounter unrepaired 8-oxo-G during chromosomal replication. Upon encountering the oxidized DNA lesion, pol δ could incorporate dAMP to induce mutagenesis. However, the higher efficiency for incorporating dCMP as the correct nucleotide predicts that genomic fidelity would be maintained by the activity of pol δ. A more likely scenario, however, involves stalling of pol δ at the lesion which would facilitate polymerase switching and allow the specialized polymerase, pol η, to replace its more faithful counterpart. The kinetic data presented here indicates that pol η is far more efficient at

replicating this oxidized lesion. As such, the higher overall efficiency for insertion coupled with a higher degree of promiscuity predicts that pol η would misinsert dAMP opposite 8-oxo-G. The higher frequency for misinsertion predicts an increase in mutagenic events associated with diseases such as cancer. Consistent with this mechanism, there are reports that overexpression of pol η in cancer cell lines correlates with resistance to chemotherapeutic agents such as cisplatin which damage DNA (38). Furthermore, pol η overexpression is a poor prognostic factor for response to chemotherapy (39). Collectively, the results of this study provide a better understanding of the complex process of mutagenesis caused by translesion DNA synthesis and offer new insights into how pol η activity may contribute to cancer initiation and progression.

This report also quantitatively evaluated if modifications to the incoming nucleotide increases the frequency of mutagenic events catalyzed by pol η during both normal and translesion DNA synthesis. Surprisingly, these kinetic studies indicate that not all nucleotide modifications adversely affect the fidelity of pol η. For example, modified nucleotides such as 8-oxo-dGTP and dITP behave as poor substrates for pol η during both normal and translesion DNA synthesis. However, certain modifications to the incoming nucleotide substantially increase the efficiency and promiscuity of pol η during the replication of oxidized DNA lesions. In this case, modified analogs such as N^6-MedATP and N^2-MedGTP are inserted opposite 8-oxo-G with remarkably high catalytic efficiencies. In fact, N^2-MedGTP is utilized ~10-fold more efficiently than either dATP or dCTP. In addition, both N^6-MedATP and N^2-MedGTP are highly high selective for insertion opposite the oxidized lesion, 8-oxo-G, compared to undamaged G. Collectively, the high insertion efficiency combined with greater selectivity for damaged DNA predicts that N^2-MedGTP is a highly pro-mutagenic nucleotide, especially when utilized by pol η during TLS.

Data generated with these modified nucleotides also provide important insights into the molecular mechanism of nucleotide selection by pol η. While it is well established that pol η is proficient at replicating bulky DNA lesions, the mechanisms underlying this activity are not completely understood. Structural data indicate that specialized DNA polymerases such as pol η possess enlarged active sites to accommodate bulky DNA lesions which cannot otherwise fit into the more constrained active sites of high-fidelity DNA polymerases (34). Based on this difference, models invoking steric fit/ shape complementarity are often used to explain the high efficiency displayed by pol η when replicating damaged DNA as well as its error-prone behavior when replicating undamaged DNA. However, it should be noted that these structural studies also highlight an important role for hydrogen-bonding interactions. This is perhaps most evident in the structure of pol η captured during the replication of a cisplatinated GG adduct (33). In this model, dCTP is properly paired with the first templating nucleobase via conventional hydrogen bonds. In general, our kinetic data favor a model invoking enthalpic contributions influenced by hydrogen bonding interactions as the primary driving force for nucleotide utilization. This is based on the fact that most modifications to hydrogen bonding groups present on the incoming dNTP produce significant negative effects on utilization by pol η during normal and translesion DNA synthesis. However, the data summarized in Table 2 show an interesting trend in which these modifications produce a more adverse effect on the efficiency of normal DNA synthesis compared to that fro replicating 8-oxo-G. This result suggests that the molecular mechanisms by which pol η replicates normal and damaged DNA are slightly different, and this may be explained by the ability of pol η to interchangeable use a combination of biophysical features, i.e., hydrogen-bonding and shape complementarity, during normal and translesion DNA synthesis. More importantly, the reliance on different biophysical features for nucleotide

selection could have important cellular consequences on genomic fidelity as pro-mutagenic replication catalyzed by pol η could be significantly enhanced by modifications to the templating nucleobase and the incoming nucleotide.

Finally, the data obtained using analogs completely devoid of hydrogen-bonding interactions (Table 3) again highlight the importance of hydrogen-bonding interactions as nearly all of these non-natural nucleotides are poorly utilized by pol η. The lone exception is 6-NITP which is utilized ~3-fold more efficiently than dATP. The increased efficiency is caused by a significant increase in binding affinity of the non-natural nucleotide (compare 4 mM to 47 mM for 6-NITP and dATP, respectively). Despite being a more efficient nucleotide substrate, 6-NITP does not show an increased selectivity for incorporation opposite the oxidized DNA lesion compared to unmodified G. This lack of selectivity unfortunately hinders using 6-NITP as a specific probe to differentiate between the replication of damaged versus undamaged DNA. A nucleotide with these properties could function as a unique diagnostic probe to detect pol η activity associated with disease initiation and development caused by hyperoxic conditions. Current efforts are underway using 6-NITP as a scaffold to generate additional non-natural nucleotides that are efficiently and selectively incorporated opposite pro-mutagenic DNA lesions.

FUNDING: This research was supported through funding to AJB from the Department of Defense (W81XWH-13-1-0238) and to SJB by National Institutes of Health Grant RO1 GM13307.

REFERENCES:

1. Echols H, and Goodman MF. (1991) Fidelity mechanisms in DNA replication. *Annu. Rev. Biochem.* **60**, 477-511.
2. Kool, E.T. (2001) Hydrogen bonding, base stacking, and steric effects in DNA replication. *Annu. Rev. Biophys. Biomol. Struct.* **30**, 1-22.
3. Kunkel, T.A. and Bebenek, K. (2000) DNA replication fidelity. *Annu. Rev. Biochem.* **69**, 497-529.
4. Indiani, C., Langston, L.D., Yurieva, O., Goodman, M.F., and O'Donnell, M. (2009) Translesion DNA polymerases remodel the replisome and alter the speed of the replicative helicase. *Proc. Natl. Acad. Sci. USA* **106**, 6031-6038.
5. Schärer, O.D. (2003) Chemistry and biology of DNA repair. *Angew Chem. Int. Ed. Engl.* 42, 2946-2974.
6. McCulloch, S.D. and Kunkel, T.A. (2008) The fidelity of DNA synthesis by eukaryotic replicative and translesion synthesis polymerases. *Cell Res.* **18**, 148-161.
7. Maga, G., van Loon, B., Crespan, E., Villani, G., and Hübscher, U. (2009) The block of DNA polymerase delta strand displacement activity by an abasic site can be rescued by the concerted action of DNA polymerase beta and Flap endonuclease 1. *J. Biol. Chem.* **284**, 14267-14275.
8. Zhong, X., Pedersen, L.C., and Kunkel, T.A. (2008) Characterization of a replicative DNA polymerase mutant with reduced fidelity and increased translesion synthesis capacity. *Nucleic Acids Res.* **36**, 3892-3904.

9. O'Day, C.L., Burgers, P.M., and Taylor, J.S. (1992) PCNA-induced DNA synthesis past cis-syn and trans-syn-I thymine dimers by calf thymus DNA polymerase delta in vitro. *Nucleic Acids Res.* **20**, 5403-5406.
10. Crespan, E., Amoroso, A., and Maga, G. (2010) DNA polymerases and mutagenesis in human cancers. *Subcell. Biochem.* **50**, 165-188.
11. Hoffmann, J.S. and Cazaux C. (2010) Aberrant expression of alternative DNA polymerases: a source of mutator phenotype as well as replicative stress in cancer. *Semin. Cancer Biol.* 20, 312-319.
12. Arana, M.E. and Kunkel, T.A. (2010) Mutator phenotypes due to DNA replication infidelity. *Semin. Cancer Biol.* **20**, 304-311.
13. Asagoshi, K., Terato, H., Ohyama, Y., and Ide, H. (2002) Effects of a guanine-derived formamidopyrimidine lesion on DNA replication: translesion DNA synthesis, nucleotide insertion, and extension kinetics. *J. Biol. Chem.* **277**, 14589-14597.
14. Wang, Z., Rhee, D.B., Lu, J., Bohr, C.T., Zhou, F., Vallabhaneni, H., de Souza-Pinto, N.C., and Liu, Y. (2010) Characterization of oxidative guanine damage and repair in mammalian telomeres. *PLoS Genet.* **6**, e1000951.
15. Forterre, P. (2013) Why are there so many diverse replication machineries? *J. Mol. Biol.* **425**, 4714-4726.
16. Johnson, R.E., Washington, M.T., Prakash, S., and Prakash, L. (2000) Fidelity of human DNA polymerase eta. *J. Biol. Chem.* **275**, 7447-7450.
17. Matsuda, T., Bebenek, K., Masutani, C., Hanaoka, F., and Kunkel, T.A. (2000) Low fidelity DNA synthesis by human DNA polymerase-eta. *Nature* **404**, 1011-1013.

18. Zhang, Y., Yuan, F., Xin, H., Wu, X., Rajpal, D.K., Yang, D., and Wang, Z. (2000) Human DNA polymerase kappa synthesizes DNA with extraordinarily low fidelity. *Nucleic Acids Res.* **28**, 4147-4156.

19. Ling, H., Boudsocq, F., Plosky, B.S., Woodgate, R., and Yang, W. (2003) Replication of a cis-syn thymine dimer at atomic resolution. *Nature* **424**, 1083-1087.

20. Vaisman, A., Masutani, C., Hanaoka, F., and Chaney, S.G. (2000) Efficient translesion replication past oxaliplatin and cisplatin GpG adducts by human DNA polymerase eta. *Biochemistry* **39**, 4575-4580.

21. Albertella, M.R., Green, C.M., Lehmann, A.R., and O'Connor, M.J. (2005) A role for polymerase eta in the cellular tolerance to cisplatin-induced damage. *Cancer Res.* **65**, 9799-9806.

22. Zhang, X., Lee, I., and Berdis, A.J. (2004) Evaluating the contributions of desolvation and base-stacking during translesion DNA synthesis. *Org. Biomol. Chem.* **2**, 1703-1711.

23. Vineyard, D., Zhang, X., Donnelly, A., Lee, I., and Berdis, A.J. (2007) Optimization of non-natural nucleotides for selective incorporation opposite damaged DNA. *Org. Biomol. Chem.* **5**, 3623-3630.

24. Motea, E.A., Lee, I., Berdis, A.J. (2012) Development of a 'clickable' non-natural nucleotide to visualize the replication of non-instructional DNA lesions. *Nucleic Acids Res.* **40**, 2357-2367.

25. Golden, J., Motea, E., Zhang, X., Choi, J.S., Feng, Y., Xu, Y., Lee, I., and Berdis, A.J. (2013) Development and characterization of a non-natural nucleoside that displays anticancer activity against solid tumors. *ACS Chem. Biol.* **8**, 2452-2465.

26. Capson, T.L., Peliska, J.A., Kaboord, B.F., Frey, M.W., Lively, C., Dahlberg, M., and Benkovic, S.J.(1992) Kinetic characterization of the polymerase and exonuclease activities of the gene 43 protein of bacteriophage T4. *Biochemistry* **31**, 10984-10994.

27. Masuda, Y., Suzuki, M., Piao, J., Gu, Y., Tsurimoto, T., and Kamiya, K. (2007) Dynamics of human replication factors in the elongation phase of DNA replication. *Nucleic Acids Res.* **35**, 6904–6916.

28. Garg, P., Stith, C.M., Majka, J., and Burgers, P.M. (2005) Proliferating cell nuclear antigen promotes translesion synthesis by DNA polymerase zeta. *J. Biol. Chem.* **280**, 23446-23450.

29. Berdis, A.J. (2001) Dynamics of translesion DNA synthesis catalyzed by the bacteriophage T4 exonuclease-deficient DNA polymerase. *Biochemistry* **40**, 7180-7191.

30. Chaney, S.G., Campbell, S.L., Temple, B., Bassett, E., Wu, Y., and Faldu, M. (2004) Protein interactions with platinum-DNA adducts: from structure to function. *J. Inorg. Biochem.* **98**, 1551-1559.

31. Alt, A., Lammens, K., Chiocchini, C., Lammens, A., Pieck, J.C., Kuch, D., Hopfner, K.P., and Carell, T. (2007) Bypass of DNA lesions generated during anticancer treatment with cisplatin by DNA polymerase eta. *Science* **318**, 967-970.

32. Zhao, Y., Biertümpfel, C., Gregory, M.T., Hua, Y.J., Hanaoka, F., and Yang, W. (2012) Structural basis of human DNA polymerase η-mediated chemoresistance to cisplatin. *Proc. Natl. Acad. Sci. USA* **109**, 7269-7274.

33. Ummat, A., Rechkoblit, O., Jain, R., Roy Choudhury, J., Johnson, R.E., Silverstein, T.D., Buku, A., Lone, S., Prakash, L., Prakash, S., and Aggarwal, A.K. (2012) Structural basis

for cisplatin DNA damage tolerance by human polymerase η during cancer chemotherapy. *Nat. Struct. Mol. Biol.* **19**, 628-632.

34. Yang, W. (2005) Portraits of a Y-family DNA polymerase. *FEBS Lett.* **579**, 868-872.
35. Fujiwara, S., Sawada, K., and Amisaki, T. (2014) Molecular dynamics study on conformational differences between dGMP and 8-oxo-dGMP: Effects of metal ions. *J. Mol. Graph Model*. **51**, 158-167.
36. Zhang, X., Lee, I., and Berdis, A.J. (2005) The use of nonnatural nucleotides to probe the contributions of shape complementarity and pi-electron surface area during DNA polymerization. *Biochemistry* **44**, 13101-13110.
37. Motea, E.A., Lee, I., and Berdis, A.J. (2013) Insights into the roles of desolvation and π-electron interactions during DNA polymerization. *Chembiochem*. **14**, 489-498.
38. Zhou, W., Chen, Y.W., Liu, X., Chu, P., Loria, S., Wang, Y., Yen, Y., and Chou, K.M. (2013) Expression of DNA translesion synthesis polymerase η in head and neck squamous cell cancer predicts resistance to gemcitabine and cisplatin-based chemotherapy. *PLoS One.* **8**, e83978.
39. Chen, Y.W., Cleaver, J.E., Hanaoka, F., Chang, C.F., and Chou, K.M. (2006) A novel role of DNA polymerase eta in modulating cellular sensitivity to chemotherapeutic agents. *Mol. Cancer Res.* **4**, 257-265.

Table 1. Summary of kinetic constants for the incorporation of natural nucleotides opposite guanine and 8-oxo-guanine by the bacteriophage T4 DNA polymerase (gp43 exo$^-$), pol δ, and pol η.

DNA	dNTP	K_m (μM)	k_{cat} (sec^{-1})	k_{cat}/K_m ($M^{-1}s^{-1}$)
T4 DNA Polymerase				
13/20G	dCTP	4.7 +/- 0.1	0.94 +/- 0.02	(1.7 +/- 0.1)*10^5
13/20G	dATP	ND	ND	ND
13/20OG	dCTP	54 +/- 16	0.59 +/- 0.07	(1.1 +/- 0.4)*10^4
13/20OG	dATP	250 +/- 40	0.76 +/- 0.13	(3.0 +/- 0.3)*10^3
Pol δ				
13/20G	dCTP	0.64 +/- 0.07	1.03 +/- 0.02	(1.6 +/- 0.5)*10^6
13/20G	dATP	ND	ND	ND
13/20OG	dCTP	34 +/- 5	0.033 +/- 0.002	(9.8 +/- 0.4)*10^3
13/20OG	dATP	258 +/- 14	0.097 +/- 0.003	(0.4 +/- 0.1)*10^3
Pol η				
13/20G	dCTP	1.3 +/- 0.3	0.88 +/- 0.10	(6.7 +/- 0.3)*10^5
13/20G	dATP	49 +/- 13	1.11 +/- 0.08	(2.2 +/- 0.4)*10^4
13/20OG	dCTP	3.0 +/- 0.6	0.40 +/- 0.02	(1.3 +/- 0.1)*10^5
13/20OG	dATP	47 +/- 7	1.13 +/- 0.06	(2.4 +/- 0.3)*10^4

Table 2. Summary of kinetic constants measured for the incorporation of natural and modified nucleotides opposite guanine (G) and 8-oxoguanine (8-oxo-G) by pol η.

Nucleotide	K_m (μM)	k_{cat} (sec^{-1})	k_{cat}/K_m ($M^{-1}sec^{-1}$)	Efficiency[a]	Selectivity[b]
13/20OG					
dATP	47 +/- 7	1.13 +/- 0.06	$(2.4 +/- 0.3)*10^4$	100%	1.14
N^6-MedATP	46 +/- 15	1.35 +/- 0.15	$(2.9 +/- 0.2)*10^4$	120%	2.23
6-Cl-PTP	137 +/- 7	0.39 +/- 0.08	$(2.8 +/- 0.4)*10^3$	12%	8.48
6-Cl-2APTP	14.3 +/- 3.2	0.09 +/- 0.01	$(6.3 +/- 0.6)*10^3$	26%	1.26
dGTP	32 +/- 10	0.25 +/- 0.03	$(7.8 +/- 0.8)*10^3$	33%	1.04
O^6-MedGTP	50 +/- 15	0.55 +/- 0.13	$(1.1 +/- 1.0)*10^4$	46%	17.2
N^2-MedGTP	0.64 +/- 0.05	0.11 +/- 0.02	$(1.7 +/- 0.1)*10^5$	720%	41
2,6-dATP	72 +/- 19	0.31 +/- 0.01	$(4.3 +/- 0.5)*10^3$	18%	11.9
dITP	64 +/- 25	0.17 +/- 0.03	$(2.7 +/-0.9)*10^3$	11%	5.6
8-oxo-dGTP	143 +/- 36	0.068 +/- 0.005	$(4.8 +/- 0.8)*10^2$	2%	2.5
13/20G					
dATP	49 +/- 13	1.11 +/- 0.08	$(2.2 +/- 0.4)*10^4$	100%	
N^6-MedATP	70 +/- 30	0.88 +/- 0.01	$(1.3 +/- 0.5)*10^3$	6%	
6-Cl-PTP	77 +/- 16	0.025 +/- 0.001	$(3.3 +/- 0.9)*10^2$	1.5%	
6-Cl-2APTP	15.9 +/- 3.9	0.08 +/- 0.01	$(5.0 +/- 0.8)*10^3$	23%	
dGTP	2.4 +/- 0.9	0.018 +/- 0.001	$(7.5 +/- 0.9)*10^3$	34%	
O^6-Me-dGTP	150 +/- 70	0.096 +/- 0.017	$(6.4 +/- 0.8)*10^2$	2.9%	
N^2-Me-dGTP	5.5 +/- 2.1	0.023 +/- 0.004	$(4.2 +/- 0.8)*10^3$	19%	
2,6-dATP	76 +/- 17	0.027 +/- 0.002	$(3.6 +/- 0.8)*10^2$	1.6%	
dITP	25 +/- 4	0.012 +/- 0.001	$(4.8 +/- 06)*10^2$	2.2%	
8-oxo-dGTP	183 +/- 41	0.035 +/- 0.003	$(1.9 +/- 0.5)*10^2$	0.9%	

Table 3. Summary of kinetic constants measured for the incorporation of non-natural nucleotides opposite guanine and 8-oxoguanine by polymerase eta.

Nucleotide	K_m (μM)	k_{cat} (sec^{-1})	k_{cat}/K_m ($M^{-1}sec^{-1}$)	Efficiency	Selectivity
13/20OG					
dATP	47 +/- 7	1.13 +/- 0.06	24,000 +/- 3,000	100%	1.09
IndTP	61 +/- 18	0.050 +/- 0.005	820 +/- 120	3.4%	3.0
5-MeITP	18 +/- 5	0.047 +/- 0.001	2,610 +/- 200	10.9%	11.6
5-EtITP	36 +/- 16	0.007 +/- 0.001	200 +/- 50	0.8%	0.24
5-EyITP	56 +/- 36	0.0015 +/- 0.0003	27 +/- 15	0.1%	0.075
5-NITP	63 +/- 12	0.344 +/- 0.020	5,460 +/- 550	23%	0.30
4-NITP	23 +/- 8	0.132 +/- 0.016	5,740 +/- 350	24%	8.57
6-NITP	3.9 +/- 1.6	0.283 +/- 0.032	72,600 +/- 1,200	303%	1.80
13/20G					
dATP	49 +/- 13	1.11 +/- 0.08	22,000 +/- 4,000	100%	
IndTP	81 +/- 18	0.022 +/- 0.001	270 +/- 80	1.2%	
5-MeITP	40 +/- 15	0.009 +/- 0.12	225 +/- 80	1.0%	
5-EtITP	10 +/- 3	0.008 +/- 0.001	830 +/- 100	3.8%	
5-EyITP	26 +/- 5	0.009 +/- 0.001	360 +/- 50	1.6%	
5-NITP	46 +/- 15	0.83 +/- 0.12	18,000 +/- 1,200	82%	
4-NITP	57 +/- 18	0.038 +/- 0.009	670 +/- 150	3.0%	
6-NITP	2.7 +/- 0.6	0.108 +/- 0.008	40,000 +/- 1,500	180%	

Figure legends

Figure 1. (A) Summary of how reactive oxygen species (ROS) can modify natural nucleobases such as guanine to generate the oxidized DNA lesions, 2,6-diamino-4-oxo-5-formamidopyrimidine (faPy-G) and 8-oxo-guanine (8-oxo-G). (B) The replication of 8-oxo-guanine can be "error-free" (dCMP insertion) or "error-prone" (dAMP insertion).

Figure 2. (A) DNA substrate used in these studies. X in the template at position 14 denotes G, C, or 8-oxo-G. (B) Denaturing gel electrophoresis images comparing dCMP insertion opposite G (13/20G) and the insertion of dCMP and dAMP insertion opposite 8-oxo-G (13/20OG) by the bacteriophage T4 DNA polymerase, pol delta, and pol eta. (C) Michaelis-Menten plots for dCMP incorporation opposite G (left panel) and 8-oxo-G (right panel) by the bacteriophage T4 polymerase. (D) Michaelis-Menten plots for dCMP incorporation opposite G (left panel) and 8-oxo-G (right panel) catalyzed by pol delta. (E) Michaelis-Menten plots for dCMP insertion opposite G (left panel) and 8-oxo-G (right panel) catalyzed by polymerase eta.

Figure 3. (A) Structures of modified purine nucleotides used in this study. (B) Michaelis-Menten plots for the insertion of N^6-MedATP opposite G (●) and 8-oxo-G (■) catalyzed by polymerase eta. (C) Michaelis-Menten plots for the insertion of N^2-MedGTP opposite G (●) and 8-oxo-G (■) catalyzed by polymerase eta. (D) Gel electrophoresis data summarizing the incorporation of modified natural nucleotides opposite G and 8-oxo-G catalyzed by pol eta. G represents guanine while OG represents 8-oxoguanine.

Figure 4. (A) Structures of non-natural nucleotides used in this study. (B) Gel electrophoresis data summarizing the incorporation of non-natural nucleotides opposite G and 8-oxo-G catalyzed by pol eta. (C) Structures of basepairs between 8-oxo-G : A, 8-oxo-G : Indole, and 8-oxo-G : 5-methyindole. In all cases, 8-oxo-G is in the *syn*-conformation

Figure 5. Hypothetical model for the coordination of pol δ and pol η activity during the replication of damaged DNA. In this model, pol δ stalls upon encountering the oxidized DNA lesion. Stalling would facilitate polymerase switching and allow pol η to replace pol δ. pol η is more efficient at misinserting dAMP opposite 8-oxo-G, and this predicts an increase in promutagenic replication. In addition, certain modified nucleotides including N^2-MedGTP are utilized more efficiently by pol η and are thus predicted to increase mutagenesis.